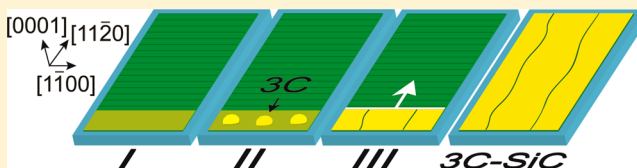


# Lateral Enlargement Growth Mechanism of 3C-SiC on Off-Oriented 4H-SiC Substrates

Valdas Jokubavicius,\* G. Reza Yazdi, Rickard Liljedahl, Ivan G. Ivanov, Rositsa Yakimova, and Mikael Syväjärvi

Department of Physics, Chemistry and Biology (IFM), Semiconductor Materials Division, Linköping University, 581 83 Linköping, Sweden

**ABSTRACT:** We introduce a 3C-SiC growth concept on off-oriented 4H-SiC substrates using a sublimation epitaxial method. A growth model of 3C-SiC layer development via a controlled cubic polytype nucleation on *in situ* formed on-axis area followed by a lateral enlargement of 3C-SiC domains along the step-flow direction is outlined. Growth process stability and reproducibility of high crystalline quality material are demonstrated in a series of 3C-SiC samples with a thickness of about 1 mm. The average values of full width at half-maximum of  $\omega$  rocking curves on these samples vary from 34 to 48 arcsec indicating high crystalline quality compared to values found in the literature. The low temperature photoluminescence measurements also confirm a high crystalline quality of 3C-SiC and indicate that the residual nitrogen concentration is about  $1-2 \times 10^{16} \text{ cm}^{-3}$ . Such a 3C-SiC growth concept may be applied to produce substrates for homoepitaxial 3C-SiC growth or seeds which could be explored in bulk growth of 3C-SiC.



## 1. INTRODUCTION

Cubic silicon carbide (3C-SiC) as well as commercially available hexagonal silicon carbide (4H- and 6H-SiC) has excellent thermal, electrical, mechanical, and chemical properties. It is very attractive for the development of metal-oxide semiconductor field-effect transistors for medium power devices,<sup>1,2</sup> high efficiency solar cells,<sup>3,4</sup> biocompatible medical devices,<sup>5</sup> or biomarkers.<sup>6</sup> Furthermore, it is a suitable substrate for the growth of nitride and epitaxial graphene layers.<sup>7,8</sup>

While technologies for producing bulk hexagonal silicon carbide ( $\alpha$ -SiC) have significantly advanced and device quality wafers have been commercially available for a number of years, the growth of bulk 3C-SiC is still lagging behind its hexagonal counterparts. The main problem hampering the progress in the growth of bulk 3C-SiC is a lack of high quality seeds which could be applied in the physical vapor transport (PVT) technique in the same way as it is done for the growth of large 4H- or 6H-SiC crystals.<sup>9</sup> Moreover, considering thermal stresses created in the seed attached to the lid or graphite plate during the PVT growth, the 3C-SiC seed with a thickness close to 1 mm would be preferable for the growth of low defect density crystals.

The 3C-SiC is usually heteroepitaxially grown on the foreign substrates such as silicon or hexagonal SiC ( $\alpha$ -SiC). Large area free-standing 3C-SiC wafers have been produced on silicon.<sup>10</sup> However, the quality of 3C-SiC is limited due to fundamental problems in the Si/3C-SiC material system. A high density of structural defects is formed in the grown crystal due to a high mismatch in thermal expansion coefficients and lattice parameters between the silicon and 3C-SiC. It was also shown that the defect density in 3C-SiC layers grown on silicon tends to saturate in the range between  $10^3$  and  $10^4 \text{ cm}^{-3}$ .<sup>11</sup> On

the other hand, the  $\alpha$ -SiC is an excellent substrate in terms of lattice parameter, thermal expansion coefficient, and chemical compatibility. However, the  $\alpha$ -SiC/3C-SiC system also possesses a fundamental problem related to the formation of structural defects called double positioning boundaries (DPBs).<sup>12</sup> The DPBs in the 3C-SiC can influence electronic properties of the material, interact with impurities, and lead to a poor behavior of a large area Schottky contacts.<sup>13,14</sup> Therefore, the reduction of DPBs density remains one of the primary goals to be achieved in the growth of 3C-SiC on  $\alpha$ -SiC substrates.

The  $\alpha$ -SiC can be roughly divided into nominally on-axis and off-oriented substrates. Nominally on-axis substrates are commonly used for heteroepitaxial growth of thin 3C-SiC layers via two-dimensional nucleation.<sup>15-18</sup> In contrast, the off-oriented substrates are the usual choice in homoepitaxial growth of 6H or 4H-SiC layers. The surface of such substrates contains a high density of steps. Therefore, incoming atoms are easily incorporated at the step kinks, and the homoepitaxial layer grows via a step flow growth mechanism.<sup>19</sup> However, under certain conditions the growth of 3C-SiC on off-oriented  $\alpha$ -SiC substrates can also be possible. The growth of thin 3C-SiC layers directly on off-oriented substrates was demonstrated using the vapor–liquid–solid (VLS) technique.<sup>18</sup> High quality but restricted area 3C-SiC epilayers have been grown using chemical vapor deposition on off-oriented 4H-SiC substrates with pre-etched mesas structures.<sup>20</sup> In contrast, larger size and bulk-like 3C-SiC layers have been demonstrated using sublimation epitaxy techniques on off-oriented 6H-SiC

**Received:** September 23, 2014

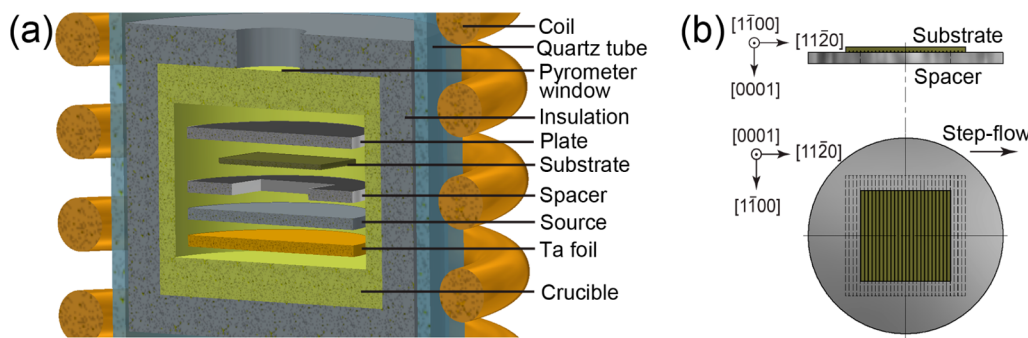


**Figure 1.** (a) Sublimation epitaxial growth arrangement. (b) Positioning of the substrate on top of the spacer.

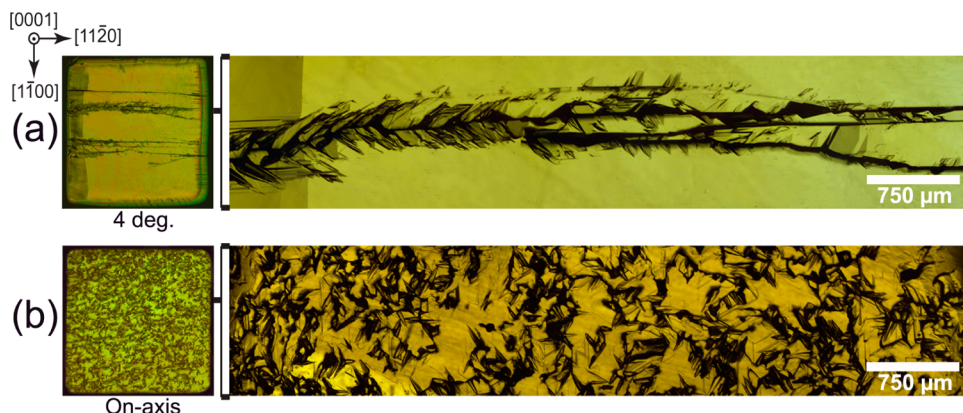


**Figure 2.** Optical micrographs of 1 mm thick 3C-SiC samples grown on 4H-SiC (0001) substrates: (a) 4 deg off-oriented, (b) nominally on-axis. The left side of the picture shows an overview of the 3C-SiC sample with a surface area of  $7 \times 7 \text{ mm}^2$ , and the right side is an enlarged view demonstrating propagation of double positioning boundaries.

substrates.<sup>21,22</sup> However, such material exhibits low crystalline quality.

The 3C-SiC growth concept that is demonstrated in this paper allows a reproducible growth of high crystalline quality thick 3C-SiC layers on off-oriented 4H-SiC substrates without foreign polytype inclusions. This concept is demonstrated using a sublimation epitaxial growth method, but the generic concept might probably also be applied to other SiC growth methods. In the case of 3C-SiC growth on conventionally used on-axis substrates, the nucleation of the cubic phase occurs in a spontaneous manner over the surface area and is difficult to control. We propose a controllable initial polytype formation and subsequent enlargement of 3C-SiC domains on off-oriented substrates leading to a significant reduction in the density of DPBs compared to the 3C-SiC layers grown on nominally on-axis substrates. Moreover, the 3C-SiC layers grown via a lateral enlargement mechanism on off-oriented substrates contain large enough DPBs-free areas which can potentially be used as seeds for the bulk 3C-SiC growth or can be explored as a substrate for homoepitaxial 3C-SiC growth for various device concepts.

## 2. EXPERIMENTAL DETAILS

The sublimation epitaxial 3C-SiC growth arrangement is depicted in Figure 1a. A graphite crucible was heated by RF generator at a frequency of 46 kHz. At elevated temperatures a solid SiC source sublimes, and vapor species (mainly Si, Si<sub>2</sub>C, and SiC<sub>2</sub>) are transferred to the substrate where they condense and form the SiC crystal. The driving force for such transfer is a temperature gradient between the source and the substrate. It has been shown that this type of

sublimation epitaxial configuration may reach a very high growth rate (up to 2 mm/h at temperatures up to 2000 °C).<sup>23</sup>

A graphite spacer with a thickness of 1 mm was placed between the source and the substrate. In all experiments, a square opening of  $7 \times 7 \text{ mm}^2$  in the spacer was used. All substrates were chemomechanically polished 4H-SiC having a 4 deg off-orientation from (0001) toward <11̄20> direction. The substrates were cut in rectangular pieces of  $10 \times 10 \text{ mm}^2$  with one of the substrate sides aligned perpendicularly to the step-flow direction. In the growth cell, the substrate was placed on top of the spacer in a way that the sides of the square shaped spacer opening, and the sides of the rectangular substrate were aligned to each other as shown in Figure 1b. Such positioning of the substrate and the spacer is a crucial element for the subsequent *in situ* formation of a large terrace at the substrate edge with an on-axis surface on which the initial 3C-SiC domains are formed before their enlargement along the step-flow direction.

Polycrystalline SiC plates were used as a source material. In addition, a tantalum (Ta) foil was inserted under the source. It acts as a carbon getter at elevated temperatures, and the growth proceeds in a silicon enriched environment which is preferable for the formation of the 3C-SiC.<sup>24</sup> A graphite plate was placed on the top of the substrate in order to prevent backside sublimation of the substrate. The temperature was measured on the top of the crucible via the opening in the insulation material using an infrared pyrometer.

Before the growth all substrates were chemically cleaned with acetone and ethanol followed by H<sub>2</sub>O:NH<sub>3</sub>:H<sub>2</sub>O<sub>2</sub> (5:1:1) and H<sub>2</sub>O:HCl:H<sub>2</sub>O<sub>2</sub> (6:1:1). Growth times up to 2 h were explored, and the growth temperature was varied from 1650 to 1900 °C. All experiments were performed in vacuum ( $10^{-5}$  mbar). The surface of the samples was characterized using an optical microscope with Nomarski interference contrast and an atomic force microscope (AFM). The crystalline quality was evaluated by high resolution X-ray diffraction (HRXRD) using Philips X'Pert HRXRD diffractometer operating in a triple axis mode with Cu Kα1 anode. In addition, low

temperature photoluminescence (LTPL) measurements at a temperature of 2 K with the samples immersed in pumped liquid helium, using as an excitation the 351 nm line of an Ar-ion laser (about 2–3 mW focused to a spot of diameter  $\sim 100 \mu\text{m}$  on the sample) were performed. The luminescence was dispersed by a monochromator (Jobin-Yvon HR 460) coupled to a CCD camera. The spectral resolution of the PL system is approximately 1 Å.

### 3. RESULTS AND DISCUSSION

In order to evaluate the reproducibility of results, a series of five 3C-SiC samples was grown on off-oriented 4H-SiC substrates using similar growth conditions (growth rate  $\approx 0.5 \text{ mm/h}$ ; growth temperature,  $1900^\circ\text{C}$ ; growth time, 2 h). A typical 3C-SiC layer obtained under the conditions mentioned above is shown in Figure 2a. The thickness of the layer is about 1.0 mm. Such a thickness is required to completely cover the  $7 \times 7 \text{ mm}^2$  surface with 3C-SiC via the lateral enlargement mechanism. A 100% surface coverage with the cubic polytype was confirmed in all samples using LTPL. The lateral enlargement growth mechanism can extend the domains several millimeters all the way from the edge, where they nucleate, to the opposite side of the sample. This leads to the formation of a 3C-SiC layer which contains only a few DPBs which propagate via the entire length of the surface along the step-flow direction (Figure 2a enlarged view). Usually single domains of up to  $2 \times 7 \text{ mm}^2$  are obtained when growing on a  $7 \times 7 \text{ mm}^2$  surface area. For comparison, we performed growth of 3C-SiC on a chemomechanically polished nominally on-axis 4H-SiC (0001) substrate using the same growth arrangement and the same growth conditions as for the sample shown in Figure 2a. As seen in panel b, the 3C-SiC layer on nominally on-axis substrate exhibit mosaic structure with high density of DPBs. A typical domain size is less than  $1 \text{ mm}^2$ , which coincides with the results reported on the growth of 3C-SiC on nominally on-axis hexagonal SiC substrates using sublimation epitaxial growth.<sup>25</sup>

The HRXRD  $\omega$  rocking curves were measured on seven different points distributed over each sample using (111) Bragg reflection and a footprint of  $1 \times 2.7 \text{ mm}^2$ . The values of the full width at half-maximum (FWHM) of  $\omega$  rocking curves on the five 3C-SiC samples grown at the same growth conditions vary from 26 to 56 arcsec (Figure 3a) with the average value in each sample being 39, 36, 48, 34, 35 arcsec. For a comparison, a mapping of FWHM of  $\omega$  rocking curves was done using the same footprint on a 3 in. commercial 3C-SiC (001) substrate which was grown on undulant silicon wafer and 4 deg off-oriented 4H-SiC substrate used in this study. The (002) and (111) Bragg reflections were used for the commercial 3C-SiC and 4 deg substrates, respectively. The average value from 22 measurement points of 105 arcsec was obtained on the commercial 3C-SiC substrate. In comparison, the measurement on the 4H-SiC substrate shows an average value of only 9 arcsec from seven measurement points. These results together with FWHM values of  $\omega$  rocking curves in various 3C-SiC samples available from the literature are presented in Figure 3b.

In order to complement the HRXRD data, we performed LTPL measurements at 2 K on the same five samples. The LTPL spectrum shown in Figure 4 is representative for all samples. It was measured in the center of the sample where the thickness of the 3C-SiC layer is about  $490 \mu\text{m}$ . It exhibits sharp and well resolved near-band-edge features, namely, the nitrogen-bound-exciton no-phonon line or zero-phonon line (ZPL) with its four phonon replicas (TA, LA, TO, and LO) as well as lines associated with multiple bound-exciton complexes

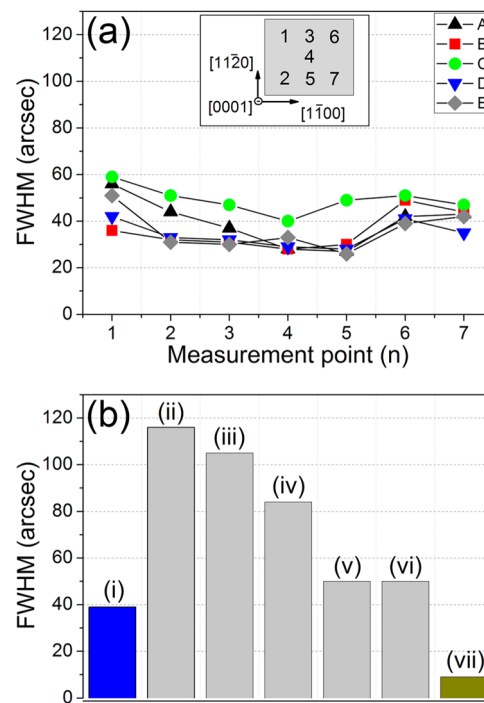


**Figure 3.** (a) FWHM values on five 3C-SiC samples grown in this study. The inset indicates measurement point position. (b) FWHM values of (i) five samples in this study (average value), (ii) homoepitaxial 3C-SiC (111),<sup>26</sup> (iii) 3 in. 3C-SiC(001), (iv) homoepitaxial 3C-SiC (001),<sup>27</sup> (v) heteroepitaxial 3C-SiC (111),<sup>26</sup> (vi) heteroepitaxial 3C-SiC (111),<sup>17</sup> (vii) 4 deg off-oriented 4H-SiC.

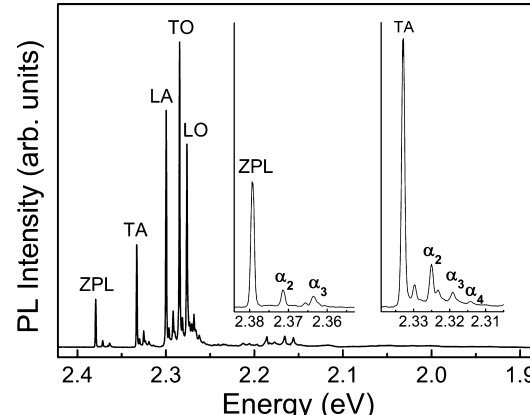


**Figure 4.** LTPL spectrum of 3C-SiC. The insets expand the regions near the ZPL and its TA phonon replica, showing the presence of multiple bound-exciton complexes.

with up to four electron–hole pairs (denoted as  $\alpha_{2-4}$ ) which indicate high quality 3C-SiC material.<sup>28–30</sup>

The intensity ratios of ZPL, TA, LA with respect to the TO line can provide information on the biaxial stress in the 3C-SiC crystal.<sup>31</sup> The LA is the line most sensitive to biaxial stress followed by LO, TA, and TO which is almost unaffected by biaxial stress.<sup>31</sup> Therefore, the intensity ratio between the LA and TO is informative biaxial stress indicator. The variations in intensity ratios of ZPL, TA, LA with respect to TO in five 3C-SiC samples grown using lateral enlargement mechanism and comparison of such intensity ratios available from the literature is presented in Table 1. The ratio between  $I_{\text{LA}}/I_{\text{TO}}$  varies in a

range of 0.74–0.80, which is indicating a low biaxial stress in 3C-SiC grown in this study.

**Table 1. Intensity Ratios of Characteristic 3C-SiC Peaks in Different Samples**

sample	$I_{ZPL}/I_{TO}$	$I_{TA}/I_{TO}$	$I_{LA}/I_{TO}$	$I_{LO}/I_{TO}$	thickness ( $\mu\text{m}$ )
this study					
A	0.17	0.34	0.75	0.70	~490
B	0.11	0.28	0.78	0.61	~490
C	0.12	0.29	0.74	0.61	~490
D	0.11	0.27	0.77	0.58	~490
E	0.09	0.25	0.80	0.53	~490
available in literature					
3C-SiC/Si <sup>31</sup> (stressed)	0.02	0.16	0.19	0.3	10.4
3C-SiC/4H-SiC <sup>16</sup>	0.2	0.41	0.67	0.73	4
3C-SiC/Si <sup>31</sup> (free film)	0.14	0.33	0.73	0.73	15
3C-SiC/6H-SiC <sup>17</sup>	0.59	0.67	1	0.67	760

We have not observed free-exciton related emissions due to the presence of residual nitrogen. The concentration of nitrogen doping can be estimated in the range of  $1\text{--}2 \times 10^{16} \text{ cm}^{-3}$  using the FWHM of TA-phonon replica, as proposed in ref 32.

The HRXRD and LTPL results indicate that the lateral enlargement mechanism allows reproducible growth of 3C-SiC layers that exhibit high crystalline quality.

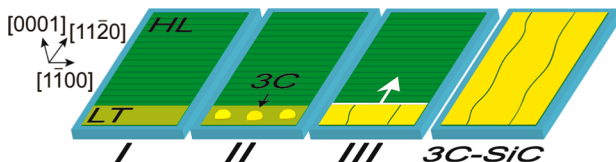


**Figure 5.** 3C-SiC formation stages on off-oriented hexagonal SiC substrate.

#### 4. GROWTH MODEL

The formation of 3C-SiC on off-oriented 4H-SiC can be divided into three interconnected stages (Figure 5): (I) Formation of a large terrace (LT) at the edge of 4H-SiC homoepitaxial layer (HL), (II) formation of the 3C-SiC domains, and (III) merging and lateral enlargement of the 3C-SiC domains along the step-flow direction. The model is generic and the thickness needed for full 3C-SiC conversion depends on the degree of off-orientation and substrate length in the  $[1\bar{1}\bar{2}0]$  direction. In order to analyze each stage presented in Figure 5, different sets of experiments were performed. For the analysis of Stage I and partly of Stage II, we have investigated an initial homoepitaxial growth of 4H-SiC which occurred during the temperature ramp-up ( $20 \text{ }^\circ\text{C/min}$ ) to 1650, 1700, 1750, 1800, and 1825  $^\circ\text{C}$ . After the targeted temperature was reached, the graphite crucible was immediately cooled down to room temperature with the cool-down rate of  $20 \text{ }^\circ\text{C/min}$ . By analyzing homoepitaxial layers formed at different temperatures, we have revealed morphological changes

in the HL which have provided information needed to explain the mechanism of the LT formation. For the analysis of Stage II and III, the 3C-SiC layers were grown at 1900  $^\circ\text{C}$  using growth time up to 2 h in order to investigate initial formation and lateral enlargement of the 3C-SiC domains.

**Stage I: Formation of a Large Terrace (LT) at the Edge of 4H-SiC Homoepitaxial Layer (HL).** The area of HL is determined by the opening in the spacer, and in these experiments it was  $7 \times 7 \text{ mm}^2$ . Considering that the HL has a rectangular shape given by the square spacer opening, the LT that evolves into an on-axis surface is always formed along the edge of the rectangular HL area which is aligned perpendicularly to the step-flow direction as shown in Figure 6a,b. Optical micrographs in Figure 6c–g show a fragment of the HL edge where the formation of the LT occurs. A dashed line in Figure 6c–g indicates a border between the substrate area that is covered by the spacer, schematically illustrated in the enlarged area of Figure 6b, and the area which was exposed to vapor species sublimed from the source.

The initial homoepitaxial growth is seen in the extract of Figure 6c, which shows that at 1650  $^\circ\text{C}$  there is no clear indication of any morphological disturbances that could be cubic polytype inclusions within the layer. At 1700  $^\circ\text{C}$  the steps at the border, indicated with a dashed line, become curved (extract of Figure 6d). Meanwhile, the rest of the HL surface contains straight steps. As the HL continues to grow, the surface at the border starts to undergo morphological changes. At 1750  $^\circ\text{C}$  a clear separation of the HL steps and the steps in the area covered by the spacer can be observed (extract of Figure 6e). As demonstrated in Figure 6b, steps at the edge, where the LT forms, have no follow-up steps, which could result in a continuous feeding of steps along the step-flow direction from the area covered by the spacer. The supply of vapor species (depicted as "Flux" in the enlarged area of Figure 6b) which could be used to create follow-up steps is blocked by the spacer. The difference in steps propagation velocities at the border marked in dashed line in Figure 6c–g induces a brake or disorder in a continuous step train structure along the edge of the HL. Consequently, the LT starts to develop. At 1800  $^\circ\text{C}$  the LT evolves into a flat/on-axis surface that is growing in a spiral mode as confirmed by the AFM in the extract of Figure 6f.

**Stage II: Formation of 3C-SiC Domains.** While the LT is still developing the 3C-SiC domains, observable with an optical microscope, start to form preferentially on the LT as seen in the sample grown at 1825  $^\circ\text{C}$ , (Figure 6g). On the basis of the surface analysis by AFM the LT surface at this stage is covered with spirals having terraces the width of which vary from 800 nm up to  $1.8 \mu\text{m}$ . In contrast, the width of step terraces in the central part of the HL, where the growth proceeds via step-flow mode, is only up to 200 nm and no 3C-SiC domains can be observed. The prioritized formation of 3C-SiC on the LT follows the nucleation theory involving the relationship between the terrace width and growth conditions, in particular, supersaturation.<sup>18</sup> Under the same growth conditions, the 3C-SiC is preferably formed on wider step terraces since the critical supersaturation level needed to form 2D nuclei of 3C-SiC is easier exceeded on wider terraces compared to the narrower ones. This explains why the initial formation of 3C-SiC domains is concentrated on the LT.

**Stage III: Merging and Lateral Enlargement of 3C-SiC Domains along Step-Flow Direction.** The 3C-SiC domains formed during Stage II merge together and cover the entire LT

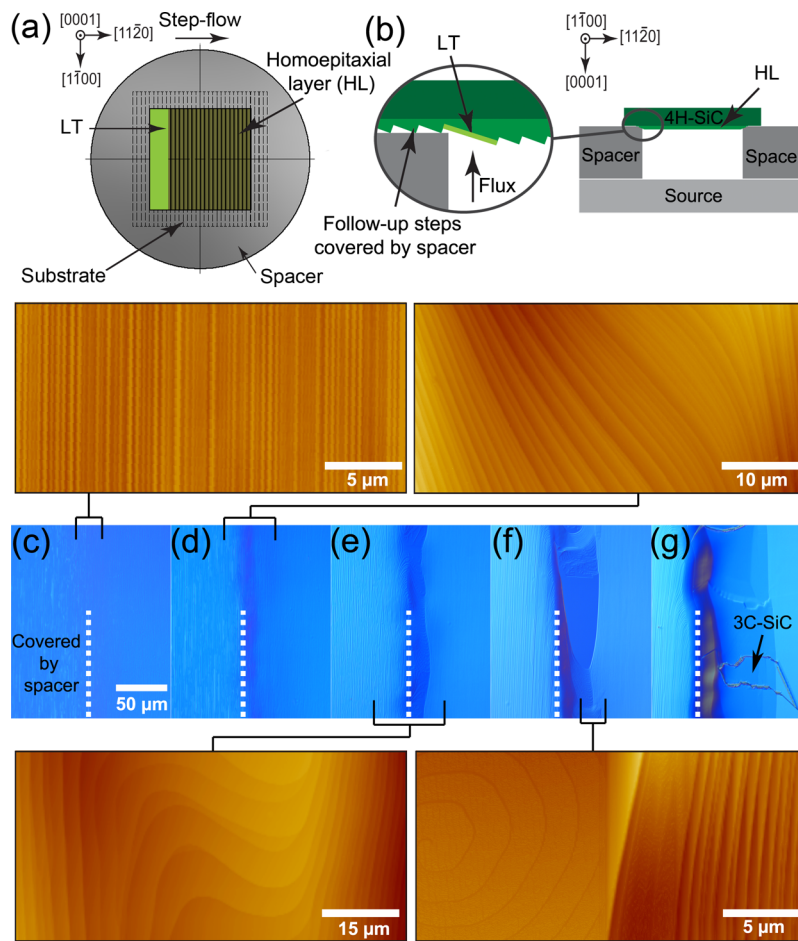


**Figure 6.** Schematic illustration of the LT position (a, b) and optical micrographs showing evolution of the LT at the edge of the HL grown during temperature ramp up to (c) 1650 °C, (d) 1700 °C, (e) 1750 °C, (f) 1800 °C, and (g) 1825 °C respectively. The enlarged areas are AFM pictures.

surface, while the rest of the sample surface remains covered with 4H-SiC growing via step-flow growth mechanism. In such way, a 3C-SiC growth front which enlarges along the step-flow growth direction is created (Figure 7). The crystalline quality of this front significantly influences the quality of the final 3C-SiC

layer. The DPBs formed on the LT propagate along the step-flow direction together with the 3C-SiC growth front. If additional/parasitic 3C-SiC domains are not present on the HL, the growth front will propagate along the step-flow direction until it reaches the opposite edge of the HL and completely covers the surface with 3C-SiC. In contrast, if the growth front collides with the parasitic 3C-SiC domains (Figure 7b,d) on the HL, it may lead to the formation of new DPBs that can cascade into further growth disturbances.

Usually, the formation of parasitic 3C-SiC domains are caused by structural defects which originate from the substrate and propagate all the way up to the surface of the HL. In addition, they could be induced by mechanical polishing scratches, presence of solid particles on the surface or various polycrystalline inclusions formed during the growth. These defects act as obstacles for the continuous flow of steps and can induce formation of parasitic 3C-SiC domains in the central part of the HL as well. Therefore, the quality of the substrate surface has to be well considered in order to obtain 3C-SiC layer with low density of structural defects.

In order to further understand the 3C-SiC enlargement mechanism, a cross-sectional analysis was made on a sample with incomplete surface coverage with 3C-SiC (Figure 8). After the formation of the 3C-SiC growth front it starts to enlarge laterally along the step-flow direction. At the same time, a transition layer starts to form and propagate between the

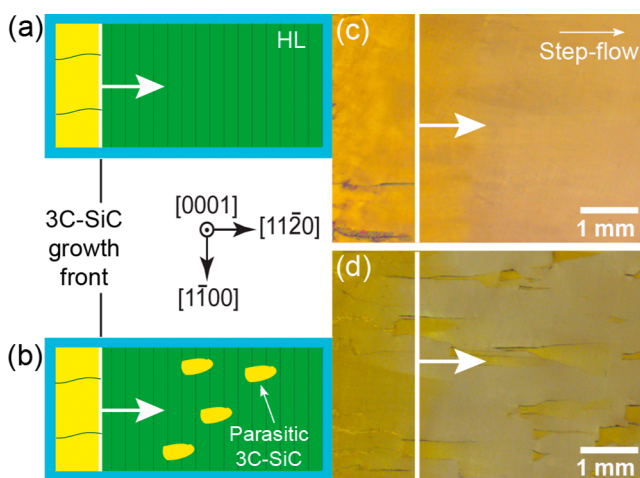


**Figure 7.** Schematic drawings and optical micrographs showing propagation of the 3C-SiC growth front (white lines in all images) without (a and c) and with (b and d) parasitic 3C-SiC inclusions on the HL.

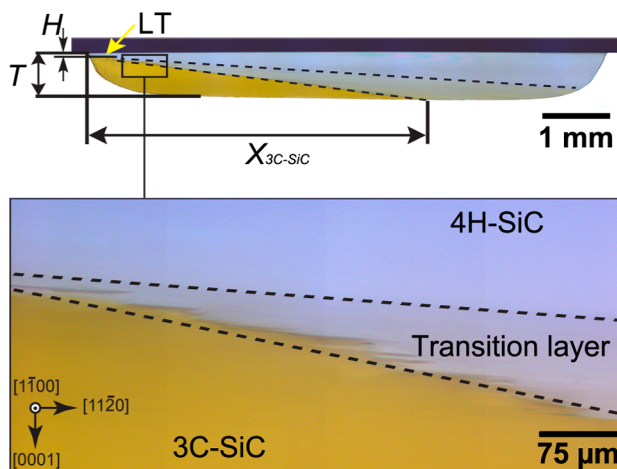


**Figure 8.** Optical micrograph of the cross sectional view of the sample with the thickness of about  $650\ \mu\text{m}$  and incomplete surface coverage with 3C-SiC.

homoepitaxial 4H-SiC and the laterally enlarging 3C-SiC layer. This occurs at a layer thickness of about  $20\text{--}30\ \mu\text{m}$ .

The approximate enlargement distance of the transition layer ( $X_{\text{tran}}$ ) (Figure 8) is proportional to the total thickness of the grown layer and inversely proportional to the tangent of the off-cut angle. Meanwhile, the approximate enlargement distance of 3C-SiC ( $X_{\text{3C-SiC}}$ ) is inversely proportional to the tangent of double off-cut angle as shown in equations below:

$$X_{\text{tran}} \approx \frac{(T - H)}{\tan \alpha}, \quad X_{\text{3C-SiC}} \approx \frac{(T - H)}{\tan 2\alpha}$$

where  $T$  is the total thickness of grown layer,  $H$  is the thickness at which LT is formed ( $20\text{--}30\ \mu\text{m}$ ), and  $\alpha$  is the off-cut angle.

The transition layer could originate due to a very small mismatch in a lattice parameter between the 3C-SiC and the hexagonal SiC substrate. A previous study of 3C-SiC grown on nominally on-axis hexagonal SiC substrates using sublimation epitaxy also revealed the existence of thin transition layer in which polytypic transformation occurred through admixture of 15R-, 6H-, and 3C-SiC and other irregular stacking sequences.<sup>33</sup> The advantage of the 3C-SiC growth on nominally on-axis substrates is that the transition layer is localized at the interface between the 3C-SiC and the substrate, and does not propagate to the growing surface. In contrast, when using off-oriented substrates the transition layer propagates to the surface and stays there until it is completely covered with 3C-SiC domains that are enlarging along the step-flow direction.

## 5. CONCLUSIONS

A series of 3C-SiC samples were grown using the same growth conditions on off-oriented 4H-SiC substrates. We have demonstrated a reproducible and well controllable growth process which allows one to obtain high crystalline quality 3C-SiC samples without foreign polytype inclusions on a surface area of  $7 \times 7\ \text{mm}^2$  and the total layer thickness of 1 mm. Single domains of up to  $2 \times 7\ \text{mm}^2$  are usually present on such size surfaces. The growth of 3C-SiC layers overpasses several interconnected stages. The 3C-SiC domains initially nucleate on an *in situ* formed large terrace with on-axis surface and subsequently laterally enlarges along the step-flow direction until a complete surface coverage with 3C-SiC is obtained. In such way, a significant reduction of DPBs compared to the

cubic polytype growth using the on-axis substrates is achieved. The surface area covered by 3C-SiC depends on the geometrical constraints, mainly on the size of the opening in the spacer and the total thickness of the layer, since an approximate enlargement distance of 3C-SiC is inversely proportional to the tangent of double off-cut angle. Therefore, this growth mechanism is generic and could be used to grow 3C-SiC layers on 4H-SiC substrates having other off-cut angles and larger substrate surfaces. This would allow one to produce even larger DPBs-free areas. The resulting 3C-SiC layers could be used as seeding layers for the bulk or homoepitaxial growth.

## ■ AUTHOR INFORMATION

### Corresponding Author

\*E-mail: valjo@ifm.liu.se.

### Funding

The Swedish Energy Agency and the Swedish Governmental Agency for Innovation Systems (Vinnova).

### Notes

The authors declare no competing financial interest.

## ■ REFERENCES

- (1) Ohshima, T.; Lee, K. K.; Ishida, Y.; Kojima, K.; Tanaka, Y.; Takahashi, T.; Yoshikawa, M.; Okumura, H.; Arai, K.; Kamiya, T. *Jpn. J. Appl. Phys.* **2003**, *42*, L625.
- (2) Schöner, A.; Krieger, M.; Pensl, G.; Abe, M.; Nagasawa, H. *Chem. Vap. Deposition* **2006**, *12*, 523–530.
- (3) Beaucarne, G.; Brown, A. S.; Keevers, M. J.; Corkish, R.; Green, M. A. *Prog. Photovoltaics Res. Appl.* **2002**, *10*, 345–353.
- (4) Richards, B. S.; Lambertz, A.; Corkish, R. P.; Zorman, C. A.; Mehregany, M.; Ionescu, M.; Green, M. A. *Proceedings of 3rd World Conference on Photovoltaic Energy Conversion*; May 11–18, 2003, Osaka, Japan; WCPEC-3 Organizing Committee, 2003; Vol. 3, p 2738.
- (5) Saddow, S. E.; Frewin, C. L.; Coletti, C.; Schettini, N.; Weeber, E.; Oliveros, A.; Jarosezki, M. *Mater. Sci. Forum* **2011**, *679* – 680, 824.
- (6) Beke, D.; Szekrényes, Z.; Balogh, I.; Czigány, Z.; Kamarás, K.; Gali, A. *J. Mater. Res.* **2013**, *28*, 44.
- (7) Masri, P.; Rouhani Laridjani, M.; Breton, O.; Averous, M. *Mater. Sci. Eng. B* **2001**, *82*, 53–55.
- (8) Yazdi, G. R.; Vasiliauskas, R.; Iakimov, T.; Zakharov, A.; Syväjärvi, M.; Yakimova, R. *Carbon* **2013**, *57*, 477–484.
- (9) Tairov, Y. M.; Tsvetkov, V. F. *J. Cryst. Growth* **1978**, *43*, 209–212.
- (10) Nagasawa, H.; Kawahara, T.; Yagi, K. *Mater. Sci. Forum* **2002**, *389*, 319.
- (11) Severino, A.; Ruggero, A.; Camarda, M.; Piluso, N.; La Via, F. *Mater. Sci. Forum* **2012**, *711*, 27.
- (12) Kong, H. S.; Glass, J. T.; Davis, R. F. *J. Mater. Res.* **1989**, *4*, 204–214.
- (13) Eriksson, J.; Weng, M. H.; Roccaforte, F.; Giannazzo, F.; Leone, S.; Raineri, V. *Appl. Phys. Lett.* **2009**, *95*, 081907.
- (14) Kohyama, M.; Yamamoto, R. *Solid State Phenom.* **1994**, *37*, 55.
- (15) Vasiliauskas, R.; Marinova, M.; Hens, P.; Wellmann, P.; Syväjärvi, M.; Yakimova, R. *Cryst. Growth Des.* **2012**, *12*, 197.
- (16) Li, X.; Jacobson, H.; Boulle, A.; Chaussende, D.; Henry, A. *ECS J. Solid State Sci. Technol.* **2014**, *3*, P75–P81.
- (17) Sun, J. W.; Ivanov, I. G.; Liljedahl, R.; Yakimova, R.; Syväjärvi, M. *Appl. Phys. Lett.* **2012**, *100*, 252101.
- (18) Soueidan, M.; Ferro, G.; Kim-Hak, O.; Cauwet, F.; Nsouli, B. *Cryst. Growth Des.* **2008**, *8*, 1044.
- (19) Kimoto, T.; Matsunami, H. *J. Appl. Phys.* **1994**, *75*, 850–859.
- (20) Powell, J. A.; Neudeck, P. G.; Trunek, A. J.; Beheim, G. M.; Matus, L. G.; Hoffman, R. W.; Keys, L. J. *J. Appl. Phys. Lett.* **2000**, *77*, 1449–1451.
- (21) Furusho, T.; Sasaki, M.; Ohshima, S.; Nishino, S. *J. Cryst. Growth* **2003**, *249*, 216–221.

- (22) Syväjärvi, M.; Yakimova, R.; Jacobsson, H.; Janzén, E. *Mater. Sci. Forum* **2001**, *353*, 143.
- (23) Syväjärvi, M.; Yakimova, R.; Tuominen, M.; Kakanakova-Georgieva, A.; MacMillan, M. F.; Henry, A.; Wahab, Q.; Janzén, E. *J. Cryst. Growth* **1999**, *197*, 155–162.
- (24) Vodakov, Y. A.; Roenkov, A. D.; Ramm, M. G.; Mokhov, E. N.; Makarov, Y. N. *Phys. Status Solidi B* **1997**, *202*, 177–200.
- (25) Yakimova, R.; Yazdi, G. R.; Sritirawisarn, N.; Syväjärvi, M. *Mater. Sci. Forum* **2006**, *527–529*, 283–286.
- (26) Vasiliauskas, R.; Marinova, M.; Syväjärvi, M.; Liljedahl, R.; Zoulis, G.; Lorenzzi, J.; Ferro, G.; Juillaguet, S.; Camassel, J.; Polychroniadis, E. K.; Yakimova, R. *J. Cryst. Growth* **2011**, *324*, 7–14.
- (27) Hens, P.; Müller, J.; Wagner, G.; Liljedahl, R.; Yakimova, R.; Spiecker, E.; Wellmann, P.; Syväjärvi, M. *Mater. Sci. Forum* **2012**, *717–720*, 177–180.
- (28) Bergman, J. P.; Janzén, E.; Choyke, W. J. *Phys. Status Solidi B* **1998**, *210*, 407–413.
- (29) Choyke, W. J.; Hamilton, D. R.; Patrick, L. *Phys. Rev.* **1964**, *133*, A1163–A1166.
- (30) Latu-Romain, L.; Chaussende, D.; Balloud, C.; Juillaguet, S.; Rapenne, L.; Pernot, E.; Camassel, J.; Pons, M.; Madar, M. *Mater. Sci. Forum* **2006**, *527*, 99.
- (31) Choyke, W. J.; Feng, Z. C.; Powell, J. A. *J. Appl. Phys.* **1988**, *64*, 3163–3175.
- (32) Camassel, J.; Juillaguet, S.; Zielinski, M.; Balloud, C. *Chem. Vap. Deposition* **2006**, *12*, 549–556.
- (33) Marinova, M.; Mantzari, A.; Polychroniadis, E. K. *Solid State Phenom.* **2010**, *159*, 39.